IBRO Neuroscience Reports 17 (2024) 290–299

Contents lists available at ScienceDirect

IBRO Neuroscience Reports

journal homepage: www.sciencedirect.com/journal/IBRO-Neuroscience-Reports

Research paper

Recovery of independent ambulation after complete spinal cord transection in the presence of the neuroprotectant polyethylene glycol in monkeys

Weihua Zhang [a,b,c,1], Shuai Ren [c,d,1], Zehan Liu [d], Mingzhe Zhang [d], Xiangchen Guan [d], Junfeng Xu [d], Xiaoping Ren [a,b,c,*]

[a] Department of Orthopedics, Ruikang Hospital Affiliated to Guangxi University of Chinese Medicine, Nanning, China
[b] Institute of Orthopedics, Ruikang Hospital Affiliated to Guangxi University of Chinese Medicine, Nanning, China
[c] Global Initiative to Cure Paralysis (GICUP), Columbus, USA
[d] Department of Orthopedics, the Second Affiliated Hospital of Harbin Medical University, Harbin, China

ARTICLE INFO

Keywords:
Spinal cord injury
Spinal cord transection
Paraplegia
Polyethylene glycol
Spinal cord fusion

ABSTRACT

Objective: Despite the conventional belief that motor function and sensation distal to the site of a complete spinal cord transection are irretrievable, our research has demonstrated significant motor recovery in mice, rats, and dogs by applying polyethylene glycol (PEG) topically via a syringe directly to the contact interface of transected spinal cord. However, before implementing this technology in human subjects, validating PEG's efficacy and enduring impact through experimentation on non-human primates is imperative.

Methods: Two 4-year-old female Macaca fascicularis monkeys underwent complete dorsal cord transection at T10. Postoperative behavioral assessment, electrophysiologic monitoring, and neuroimaging examinations were recorded, and tissues were obtained for histological examination at the end of study.

Results: The monkey whose spinal cord had been fully transected in the presence of PEG developed useful recovery already at 3 months and near-complete recovery of motor function in the hind-limbs at 18 months. The control animal without PEG remained paralyzed. Cortical somatosensory evoked potentials recovered postoperatively only in PEG-treated monkey vs none in the control. Diffusion tensor imaging showed re-establishment of continuity of the white matter in PEG-treated monkey, but not in the control. Moreover, histology revealed intact neuronal bodies, axons, and myelin tissue at the spinal cord transection site in PEG-treated monkey only.

Conclusion: This report suggests that in primates, an acutely transected spinal cord can be re-fused in the presence of PEG with restoration of neural continuity and functional recovery of motor activity distal to the site of transection.

1. Introduction

Despite of over a century of intensive research, the recovery from paralyzing spinal cord injuries (SCIs) remains incurable. Contemporary engineering solutions, ranging from exoskeletons tailored for lower dorsal SCIs to brain-computer interfaces and electrical spinal cord stimulation, have fallen short in fully restoring normal sensory-motor function (Ahuja et al., 2017). The imperative for a biologically-rooted intervention capable of reinstating functional neural continuity has become increasingly apparent.

Among the spectrum of SCIs, spinal cord transection (SCT) stands out as the most severe form, invariably entailing complete and enduring motor and sensory deficits in affected individuals. A breakthrough came in 2013 with the formulation of the GEMINI spinal cord fusion (SCF) protocol, offering a novel avenue for reestablishing neurophysiological conduction across acutely severed spinal cords, even in completely transected spinal cords (Canavero, 2015). This pioneering biologic approach entails the immediate bathing of the transected spinal cord stumps in a neuroprotective and fusion-inducing solution composed of polyethylene glycol (PEG), followed by electrical stimulation of the

* Correspondence to: Department of Orthopedics, Ruikang Hospital Affiliated to Guangxi University of Chinese Medicine, Huadong Road 10, Xingning District, Nanning, Guangxi 530011, China.
E-mail address: chinarenxg@126.com (X. Ren).
[1] First co-author.

https://doi.org/10.1016/j.ibneur.2024.09.005
Received 23 July 2024; Received in revised form 25 September 2024; Accepted 25 September 2024
Available online 26 September 2024

spinal cord precisely at the point of controlled and sharp SCT. The outcome manifests PEG can promote fusion of nerve populations across the transection site and immediately restore electrical conductivity. Intriguingly, this protocol also demonstrates the viability of gray matter interneurons, with subsequent axonal sprouting across the fused interface (Canavero et al., 2016). PEG is a non-toxic substance with a wide range of clinical and pharmaceutical applications, including several PEGylated drugs. PEG is also FDA-approved for use as a preservative additive before organ transplantation (Pasut et al., 2016). PEG's neuroprotective attributes, coupled with its capacity to induce membrane resealing, have been unequivocally demonstrated in various studies. The heightened fusogenic capability of PEG serves as a countermeasure against the generation of free radicals, which are recognized instigators of cellular injury. Notably, this protective action encompasses the attenuation of reactive oxygen species induction and lipid peroxidation subsequent to SCI (Luo et al., 2002).

Patients who experience traumatic SCIs resulting in functionally complete transections often receive treatment hours after the trauma, by which time inflammation and swelling have set in. These processes can eventually lead to scarring and fibrosis, creating a barrier that prevents any neural regrowth across the site of the spinal injury and subsequently results in permanent paralysis distal to the injury site. To address this challenge, we have designed an surgical procedure to tackle this problem. After removing scar tissue, we excise half of the spinal cord tissue, preserving one side of the posterior spinal artery, and transplant it from the distal spinal cord to bridge the gap between the distal and proximal spinal cord stumps, ensuring the maintenance of its arterial supply (Ren et al., 2021). In this context, the GEMINI protocol stands out as a promising candidate for spinal cord fusion (SCF). Recent years have witnessed a sequence of experiments conducted by our team in mice, rats, and dogs (Ye et al., 2016; Kim et al., 2017; Ren et al., 2017; Liu et al., 2018; Ren et al., 2019a), and by other researchers in pigs, which provide robust support for the rationale underlying the GEMINI protocol (Ren et al., 2019b). However, before considering the translation of these findings to human application, primate data will be invaluable to corroborate and advance these outcomes. This study thus presents compelling evidence by evaluating the PEG arm of the GEMINI protocol in a primate model, contributing a crucial step toward potential human translation.

2. Methods and materials

The primary objective of this study was to conduct a comparative analysis of motor and sensory recovery between two monkeys. One monkey underwent an operative complete transection of the spinal cord at the T10 level, with the transected cord ends treated using the neuroprotective substance PEG-600, while another monkey experienced a similar transection without the administration of the neuroprotectant fusogen. Subsequently, close monitoring was implemented to assess the emergence of motor function in the lower extremities, the restoration of urinary control, and the presence of sensory function, as evaluated through somatosensory evoked potential testing. These assessments served as tangible indicators of both descending and ascending neural transmission across the site of SCT.

The inclusion of only two monkeys in this study was determined by multiple considerations. Firstly, our research team has conducted an extensive series of systematic experimental studies focusing on PEG treatment within several SCT models encompassing mice, rats, and beagle dogs. The experimental investigation involving these two monkeys plays a pivotal role in validating the potential clinical translation of PEG treatment for spinal cord injuries. Secondly, the ethical implications inherent in animal research prompted us to judiciously limit the number of subjects used, reflecting our commitment to upholding ethical standards while ensuring the scientific robustness of the outcomes.

All procedures conducted in this study received approval from both the Institutional Animal Care and Use Committee of Harbin Medical University (HMUIRB-2008–06) and the Institute of Laboratory Animal Science of China (A5655–01), in strict adherence to Directive 2010/63/EU of the European Parliament. Animal data reporting followed The ARRIVE 2.0 guidelines. For this study, two female Macaca fascicularis, aged four years, were procured from Suzhou Xishan Zhongke Laboratory Animal Co., Ltd (Suzhou, PRC). The animals were provided a comfortable housing environment, adhering to a light/dark cycle of 12 hours each, and were provided with ad libitum feeding.

2.1. Operative procedure for spinal cord transection

Upon establishing intravenous access, a dose of ketamine at 0.1 ml/kg was administered intravenously to induce general anesthesia, followed by endotracheal intubation to facilitate artificial ventilation. Anesthesia was maintained through intravenous administration of propofol at 10 mg/kg·h, remifentanil at 0.2 μg/kg·min, and vecuronium at 0.1 mg/kg. The subjects were placed in the prone orientation, with subsequent placement of the evoked potential electrodes (as specified below).

Sequentially, the skin, subcutaneous fat, and underlying musculature covering the spine were incised in layers. Laminectomy was meticulously performed using specialized spinal surgical instruments at the thoracic 10 (T10) level. Employing microscopic guidance, an incision was made in the dura mater, followed by gentle elevation of the spinal cord at the T10 level with a custom hook fashioned from a Kirschner wire (1−0). Complete transection was achieved utilizing a sapphire blade (Shanghai Jingming Fine Technology Co., LTD., China). Prior to the transection, vasoconstriction was induced using a solution of cold saline (4 ℃) augmented with epinephrine to reduce bleeding. Notably, no gap was created between the ends of the transected spinal cord. Subsequent to the transection, a volume of PEG-600 (100 % w/v, Sigma-Aldrich/Merck, Germany) at 5 ml or 0.9 % NaCl at 5 ml was applied topically via a syringe directly to the contact interface of transected spinal cord (Control V.S PEG-treated), and it was left undisturbed in its application. The dura mater was then sutured shut without aspirating the administered fluid, and the wound was subsequently closed layer by layer using standard procedures.

2.2. Postoperative care

The monkeys were accommodated comfortably within spacious veterinary cages. Intravenous Cefoperazone Sodium and Sulbactam Sodium (25 mg/kg; Harbin General Pharmaceutical Factory's Sales Company, Harbin, Heilongjiang, PRC) were administered for 3 consecutive days. Throughout the study period, a diverse and nutritious diet was administered under the close supervision of our veterinary experts. Daily routines incorporated hip massage and lower limb rehabilitation protocols. Furthermore, a selection of soothing music was provided during daily hours. To prevent the development of pressure sores, suspension chairs were employed. Urinary catheterization was undertaken until sphincter function recovery was achieved.

2.3. Evaluation of hindlimb motor function

The animals underwent a comprehensive battery of neurological assessments at regular intervals following SCT. Motor function evaluation encompassed regions distal to the site of SCT. To gauge the progress in motor function within the lower limbs innervated by nerves traditionally believed to originate proximal to the SCT site, two distinct evaluation scales were employed. The first was a widely adopted, modified 5-point Tarlov scale, while the second was a more detailed 21-point scale (Sledge et al., 2013) developed by Pritchard et al. in a monkey hemisection model of SCI.

Assessment of hindlimb function was conducted both preoperatively and postoperatively on days 1, 7, 15, 30, 90, 180, 360, and 540 after the

SCT procedure. Quadrupedal locomotion was systematically recorded via wide-field and close-up video recordings, conducted within a standard cage and a controlled laboratory room, respectively. Each video session spanned a continuous 5-minute duration and was conducted twice (cage + room) on each evaluation day. The camera's field of view was optimized with appropriate illumination for enhanced recording. Instances of upright standing and cage climbing were documented using food rewards.

The subsequent evaluation of video data was undertaken by an impartial reviewer, uninvolved in the in vivo execution of the study, thus maintaining blinding. Ratings for each video session were derived from meticulous analysis of all recorded segments, encompassing both wide-field and close-up footage. These ratings culminated in an overall observational neuromotor score for each hind limb, independently.

2.4. Neurophysiology

Cortical somatosensory evoked potentials (SSEPs) were recorded immediately after the induction of anesthesia and subsequently at 3, 5, and 7-minute intervals following spinal cord transection (SCT), as well as after the application of either PEG or saline for bathing. The recorded data were analyzed by Lab Chart software (AD Instruments, Bellavista, Australia). The stimulating electrode was accurately positioned over the right sciatic nerve, while the recording electrode was placed over the sensory cortex. Stimulation parameters encompassed 30 mA, 200 ms duration, and a frequency of 0.25 Hz. The waveform changes of P1–N1 and the latency of P1 were observed.

2.5. Neuroimaging

Both animals underwent Magnetic Resonance Imaging (MRI) and Diffusion Tensor Imaging (DTI)(15−17) using a 3.0 T MRI system (Achieva 3, Philips, Amsterdam, The Netherlands). The imaging procedures were performed with the animals in a prone position under ketamine anesthesia. Sagittal T2-weighted Fast Spin-Echo (TR = 1700 ms; TE = 100 ms; slice thickness = 3 mm; slice gap = 0.1; NSA = 4) and axial single-shot Echo-planar DTI (TR = 6100 ms; TE = 93 ms; voxel size = 2 mm x 2 mm; slice thickness = 2 mm; slice gap = 0; NSA = 2; diffusion direction number = 15). These imaging sequences were acquired at three time points: 1 month, 6 months, and 18 months postoperatively for the treated animal, and at 1 month only for the control animal. Furthermore, the DTI original images underwent processing to generate color DTI maps.

2.6. Histology

At the end of the study (18 months for the experimental animal and 1 month for the control), each animal was subjected to anesthesia, and the spinal cord was exposed as previously described. Subsequently, a local perfusion was performed using a solution of 0.9 % NaCl and 4 % paraformaldehyde. Immediately thereafter, the spinal cord tissue at the T10 level was excised. The animals were euthanized through intravenous administration of sodium pentobarbital (100 mg/kg). Small tissue samples ($<1\ mm^3$) were removed from the middle of the fusion area for electron microscopy analysis. The entire tissue block was then immersed in a 4 % paraformaldehyde solution for 36 hours. Subsequently, a gradual alcohol dehydration process was employed, followed by embedding the tissue in paraffin. The cord was studied on transverse 5 μm slices at the site of transection. Paraffin sections were then de-waxed with xylene and then hydrated by passing through decreasing concentration of alcohol baths and water for staining with H&E, Cresyl Violet (CV/ Nissl) and Luxor Fast Blue (LFB). Finally, dehydration in increasing concentration of ethanol and clearing in xylene completed the procedure. CV stains neurons by binding to the Nissl substance present in neuronal bodies and their nuclei (but not in axons and axon hillocks), whereas LFB stains myelin. All sections were visualized on an Olympus BX53-FL digital fluorescence microscope (Tokyo, Japan).

2.7. Immunohistochemistry

After deparaffinization, the sections were quenched with endogenous peroxidase activity for 30 min in 3 % methanol hydrogen peroxide. The antigen (https://www.abcam.com/protocols/ihc-fixation-protocol) was then fixed in a microwave buffer in citrate buffer (pH: 6.0) for 5 min. The sections were incubated with primary antibodies to Neurofilament-200 (NF-200, 1:50, Abcam, USA) and to Myelin Basic Protein (MBP, 1:50, Invitrogen, USA) overnight at 4°C. Thereafter, the secondary solution (PV secondary antibody kit, Beijing Zhongshan Jinqiao Biotechnology Co., Ltd.) was incubated at 37°C for 20 min in darkness. The DAB dye solution was added drop-wise. Finally, the sections were mounted on slides for microscope observation after hematoxylin counterstaining, dehydration, and clearing in xylene. Positive staining tissue of NF-200 and MBP was quantified through morphometric image analysis (integrated optical density, IOD) with the aid of acquired fluorescent photomicrographs, utilizing the Image J software (National Institutes of Health, Bethesda, MD).

2.8. Transmission electron microscopy (TEM)

The tissue samples harvested from the fusion zone were cut into small pieces and placed in 2.5 % glutaraldehyde at 4°C overnight. Fixation with 1 % citric acid followed for 1.5 h. The samples were dehydrated by gradient acetone and embedded in an epoxy resin-embedding agent overnight, followed by polymerization at 80°C for 48 h. The sample was cut into ultra-thin sections (75 nm) using an ultramicrotome (EM UC6, Leica Microsystems, Germany) and stained with uranyl acetate and lead citrate. An 80 KV TEM was used to visualize the samples (Hitachi, H-7650, Japan).

2.9. Pain assnessment

Although this study was exclusively geared toward evaluating motor recovery, observers were also instructed to assess the presence of any possible signs of central pain of cord origin (Canavero and Bonicalzi, 2018). At present, there are no universally accepted methods to assess chronic pain in nonhuman primates; however, there is a consensus that screams or moans, decreased feeding and drinking, aggression, prolonged crouching, "sad" facial expressions or grimaces, and abstaining from grooming are all signs of possible pain (Institute of Laboratory Animal Resources U.S., 1992). Evoked pain was not assessed quantitatively (e.g. heat pain sensation using a standard thermode), but at the end of the follow-up, ice-cold compresses were applied to all four limbs in order to elicit cold allodynia; whenever pain is produced, a response of intense screams or grimaces is expected.

3. Results

Every possible measure was taken to ensure the well-being of the animals, aiming to minimize any potential discomfort. Vigilance by our veterinary experts ensured the absence of bed sores, while a diverse and nutritionally rich diet was administered. Postoperatively, both monkeys experienced paraplegia and urinary retention (as detailed in the "Postoperative Care" section above). Regrettably, because there was absolutely no degree of motor or sphincter recovery (Fig. 1 D-F), and the animal appeared to be in distress due to the severe kyphosis worsened by the sitting posture (Fig. 3 D1), the control monkey was humanely euthanized within the first month post-operation. This decision was made in consideration of the animal's distress and quality of life.

3.1. Motor recovery

The control monkey exhibited a Tarlov score of 0 and a B-21

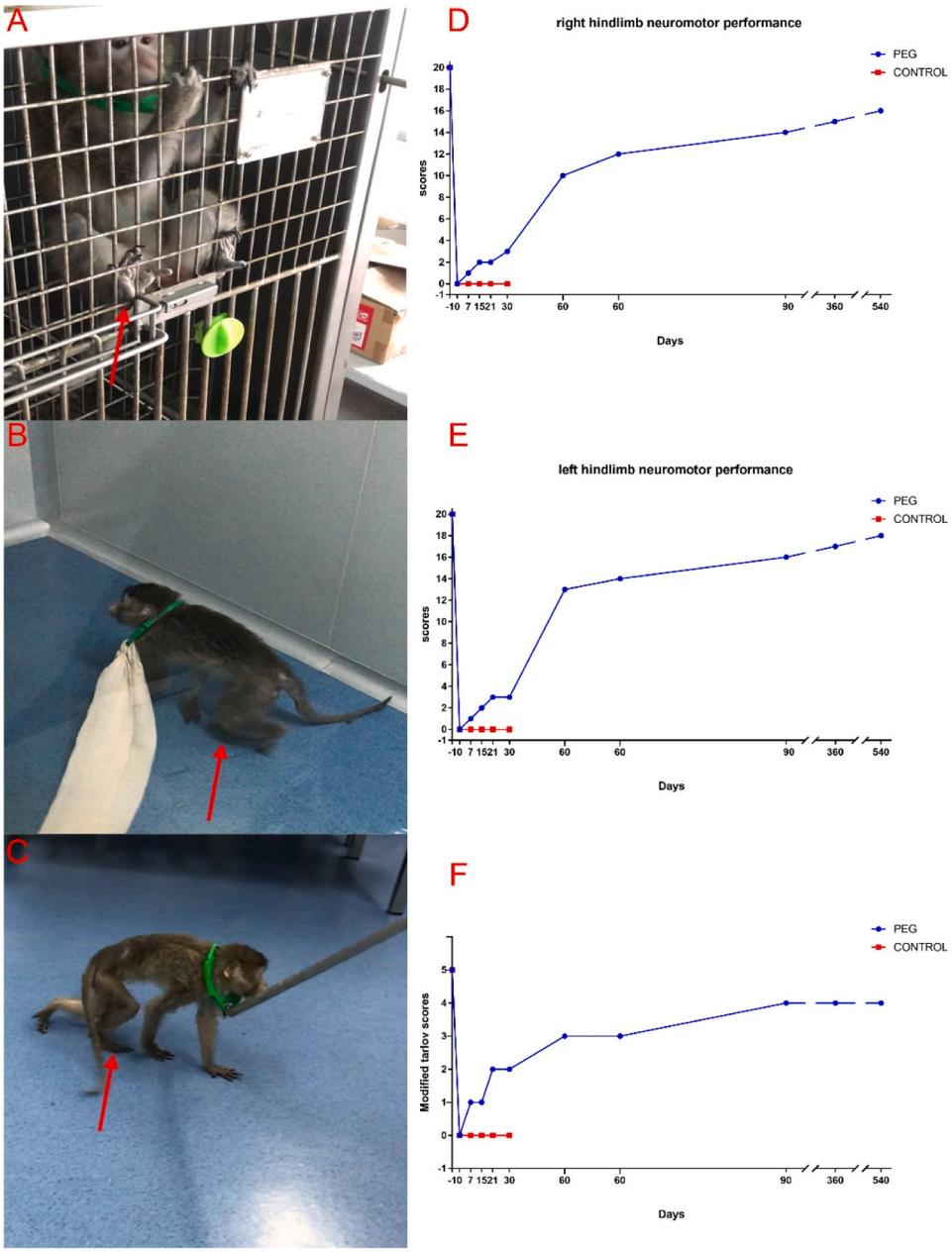

Fig. 1. Progression of recovery at 6 months (A), 12 months (B) and 18 months (C). Notice how hindlimbs clear the floor during voluntary ambulation (arrow: right hindlimb). Recovery plotted on the Pritchard 21 point scale (D: right limb, E: left limb) and modified Tarlov scale (F).

(Pritchard) score of zero at the one-month, signifying an absence of motor function. Remarkably, no motor activity was observed in the hind limbs of this monkey postoperatively. In contrast, the PEG-treated monkey displayed intermittent voluntary movements in the hind limbs just 7 days post-surgery. By the first month, frequent movements were noted, allowing the animal to assume a squatting position, although weight-bearing was not attainable. During ground testing, the forelimbs primarily propelled the PEG-treated animal, with the hind limbs showing some coordinated movement. During cage climbing, the hind limbs were at times dragged, yet propulsive movements were occasionally noticeable. Progressing to the third month, the hind limbs were able to support body weight, and initial attempts at climbing were observed. Although the forelimbs remained the primary propulsive force during ground movements, the hind limbs contributed intermittently, displaying decently coordinated movements. When climbing, the hind limbs were placed appropriately on the bars, albeit with some coordination challenges. Reaching the sixth month, all four limbs exhibited harmonious coordination, and substantial recovery of muscle strength in the hind limbs allowed for locomotion. Nevertheless, a disparity was noted between the left and right hind limbs – while the left foot executed coordinated flexion and extension, the right foot only demonstrated flexion without extension. During cage climbing, coordination was generally well-maintained, though sporadic uncoordinated movements were observed, characterized by flexion without extension (Fig. 1 A). This coordination progress continued on from 12-month (Fig. 1 B) to 18-month (Fig. 1 C) (Video 1). The PEG-treated monkey achieved Pritchard Scale scores of 16 and 18 out of 20 on the right and left sides, respectively (Fig. 1 D, E), along with a modified Tarlov Scale score of 4 out of 5 (Fig. 1 F). Sphincter control was swiftly regained within a month, albeit with some persistent stress incontinence throughout the follow-up period. Importantly, it is noteworthy that there were no indications of chronic pain throughout the entire duration of follow-up.

Supplementary material related to this article can be found online at doi:10.1016/j.ibneur.2024.09.005.

3.2. Somatosensory evoked potentials

Cortical sensory evoked potentials (cSSEPs) were normal before SCT in both animals (Fig. 2 A1, B1). However, after SCT, the control animal failed to elicit any normal cortical response upon sciatic nerve stimulation at all observed time points (3, 5, and 7 minutes later; Fig. 2 A2-A4). In contrast, the experimental monkey treated with PEG displayed the emergence of a normal cortical P1 wave at 3 and 5 minutes after SCT/PEG treatment, maintaining its normalcy at the 7 minutes (Fig. 2 B2-B4).

3.3. Neuroimaging

One month after the surgery, DTI analysis revealed a lack of white matter continuity in the control monkey (Fig. 3 D2, D3), with a distinct gap seen on T2-weighted images (T2WI) (Fig. 3 D1). In contrast, the PEG-treated monkey demonstrated a rapid re-establishment of white matter continuity, evident at one month (Fig. 3 A2, A3), more prominently at six months (Fig. 3 B2, B3), and consistently maintained at 18 months (Fig. 3 C2, C3). Notably, T2WI of the PEG-treated animal did not exhibit any gap (Fig. 3 A1-C1).

Both monkeys exhibited kyphosis on postoperative T2WI. In the PEG-treated monkey, the Cobb angle of kyphosis measured 34° at one month post-surgery, to 38° at six months, and further to 42° at 18 months (Fig. 3 A1-C1). Conversely, due to the absence of hind limb motor function recovery in the control, the Cobb angle of kyphosis reached 46° after only one month (Fig. 3 D1).

3.4. Histology, immunohistochemistry, and transmission electron microscopy (TEM)

At the end of follow-up (1 month for the control and 18 months for the experimental animal), histologic, immunohistochemical and TEM evaluation of the fusional interface was performed. In terms of H&E and Nissl staining, intact neuronal bodies could be seen only in the cord tissue of PEG-treated monkey (arrows in Fig. 4 A, C), but not the control (Fig. 4 B, D). Moreover, in the LFB staining, the healthy myelin tissue in the PEG-treated monkey could be clearly observed in the shape of a circle (arrows in Fig. 4 E), while in the control group, there was almost disorganized structure myelin tissue. Similar results were observed in immunohistochemical staining, where NF-200-positive axons and MBP-positive myelin sheathe were observed in the spinal cord of PEG-treated animal (arrows in Fig. 5 A, C), whereas few were observed in the control (Fig. 5 B, D). The positive staining densities of NF-200 and MBP in the PEG-treated animal were significantly higher than that in the control (Fig. 5 E, F). On TEM, Broken and loosely myelinated tissue was found in the tissue of the spinal cord transection in both PEG and control animals, especially in the control (square+arrows in Fig. 6 C, D). However, relatively less disorganized myelinationand more newly myelinated tissue were observed in the PEG-treated animal (circle+arrows in Fig. 6 C, D).

4. Discussion

Consistent with prior studies conducted in rodent and canine models (Ye et al., 2016; Kim et al., 2017; Ren et al., 2017; Liu et al., 2018; Ren et al., 2019a, 2019b), this present experimental case report substantiates the notion that the application of the neuroprotective agent PEG to an acutely transected spinal cord can lead to a notable "re-fusion" phenomenon and unprecedented levels of motor recovery, but in a primate model. It is noteworthy that PEG treatment alone has shown superiority over a range of strategies tested in experimental rodent and canine spinal cord transection models. These encompass various interventions such as diverse types of stem cells, olfactory ensheathing glia, scaffolds, and other methodologies (Ren et al., 2019b). For comparative context, a non-sham-controlled study involving grafting of human fetal spinal cord-derived neural progenitor cells after a C7 hemisection reported a modest improvement exceeding 25 % in objective manipulation scores in four out of five monkeys (compared to one of four controls exhibiting such an improvement), accompanied by a 12 % enhancement in climbing score commencing several months after grafting (Rosenzweig et al., 2018). Contrasting these outcomes to the current study, the PEG-treated monkey displayed occasional voluntary movements of the hind limbs 7 days postoperatively. Additionally, coordinated movements and locomotion were all observed within 6 months after SCT. The ultimate scores in both Pritchard Scale and Tarlov Scale almost reached the full points, representing an unprecedented levels of motor recovery. Most importantly, this is a recovery from a complete T10 transection instead of hemisection. Thus, the present case yielded substantially superior results with much faster onset of the treatment (Fig. 1).

Neuroimaging and histological analysis of the experimental animal underscored the occurrence of neural fiber fusion and regeneration at the transection interface, thereby offering a plausible rationale for the observed motor recovery (Figs. 3–5). Our current findings align with our prior quantitative investigations in rodent and canine models, in which neuroprotective effects of PEG has also been clearly demonstrated (Ye et al., 2016; Kim et al., 2017; Ren et al., 2017; Liu et al., 2018; Ren et al., 2019a). In those studies, we observed minimal vacuolization attributed to tissue injury (cystic regions) within spinal cords treated with PEG, exhibiting a marked and statistically significant distinction from the control group. Moreover, PEG-treated animals demonstrated abundant myelin staining in contrast to the limited staining observed in the controls. Furthermore, in the control group, evident signs of Wallerian degeneration were pronounced both above and at the spinal cord transection site, inclusive of the course of corticospinal fibers. In contrast, treated animals exhibited, on the contrary, considerable preservation of fibers, which were notably observed traversing the fusion interface through the scar tissue. The veracity of this spinal cord crossing and fusion was corroborated by immunolabeling of the NF protein (NF200), revealing substantial axonal sprouting spanning the spinal cord transection site. The outcomes we present here in the primate context closely mirror findings in rodent and canine models, thereby reinforcing the consistency of our observations.

The impediment of scarring has been prominently recognized as a pivotal factor obstructing the successful regeneration of the spinal cord, hindering neural transmission encompassing both motor and sensory

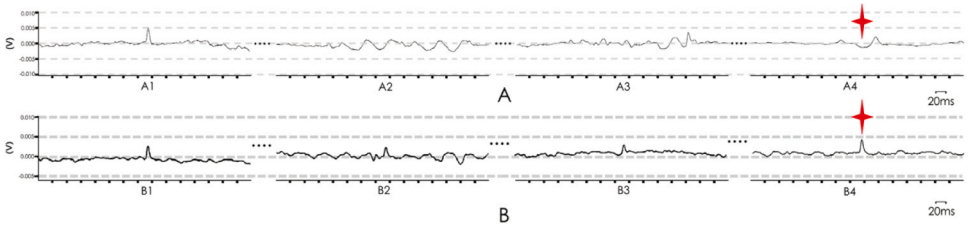

Fig. 2. SSEP tracings: preoperatively (A1: control; B1: PEG), at 3 (A2: control; B2: PEG), 5 (A3: control; B3: PEG) and 7 (A4: control; B4: PEG) minutes post-treatment. Signal conduction was restored in the PEG-treated monkey as early as 7 minutes after PEG fusion, but not in the control.

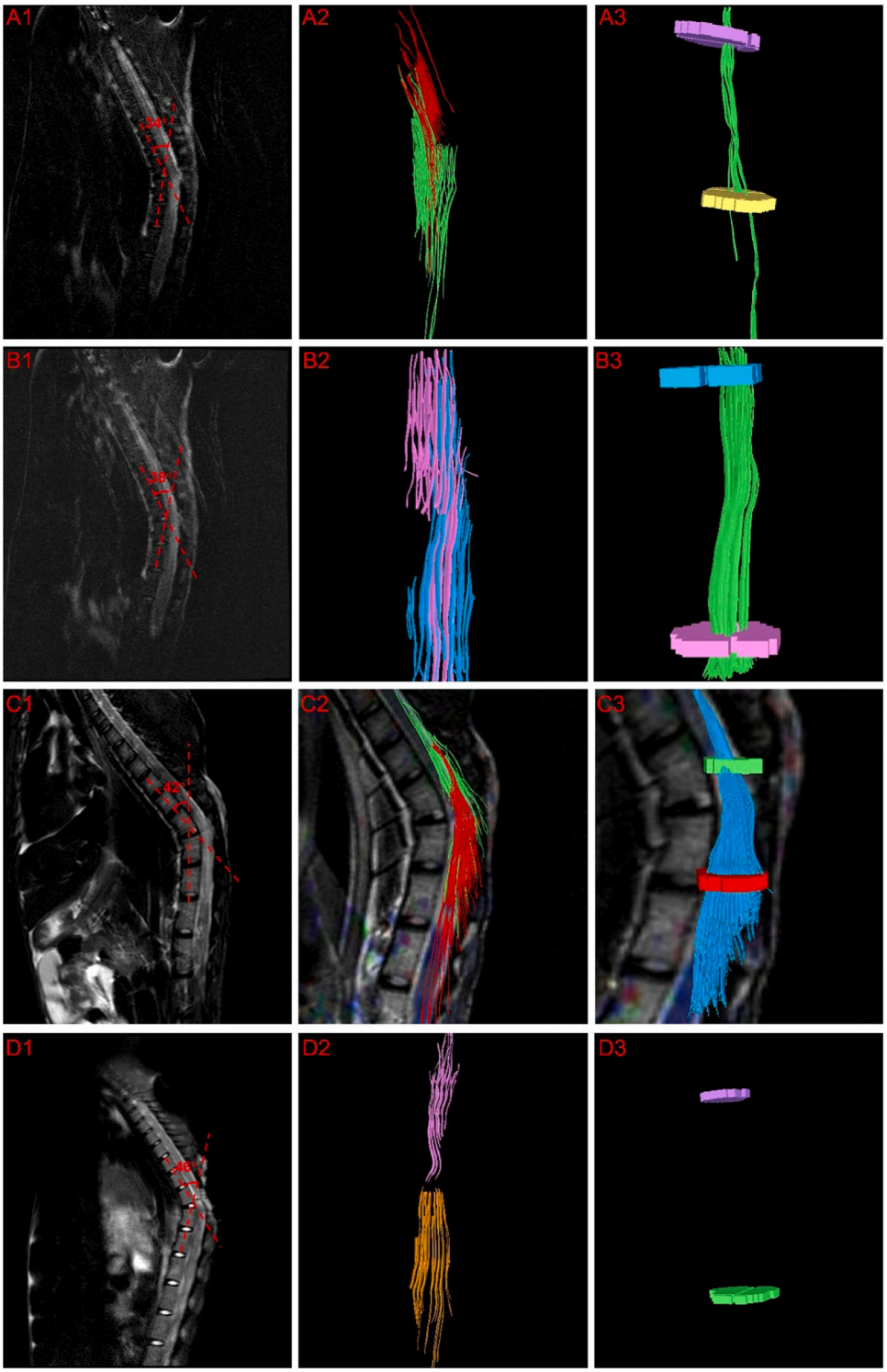

Fig. 3. Postoperative T2WI and DTI images of two monkeys. Postoperative T2WI showed the presence of kyphosis in both monkeys (A1, B1, C1, D1). T2WI of the PEG-treated monkey at 1 month (A1), 6 months (B1) and 18 months (C1) after surgery showed normal signal intensity at the spinal cord transection and no significant vacuolization. The plane of transetion at T10 was observed in T2WI of the control monkey at 1 month after surgery (D1). Nerve fiber continuity was restored on postoperative DTI imaging in the PEG-treated monkey (A1, A2, B1, B2, C1, C2) but not in the control monkey (D1, D2).

functions across the transection site, and compromising the recovery of motor abilities and sensory perception. Notably, PEG did not influence scarring in either our current study or our previous investigations (Kim et al., 2017; Ren et al., 2019a). However, within this primate model, PEG was promptly applied immediately after the spinal cord was transected. The acuity of the transection meant that astrocytic scarring and inflammation, both known hindrances, were not yet established, as such scarring typically becomes evident approximately 2–3 weeks following injury. Additionally, the employment of an extremely sharp spinal cord transection minimized collateral trauma and resultant inflammation, resulting in a scarcity of necrotic or devitalized tissue that could impede the regenerative process or the potential fusion of

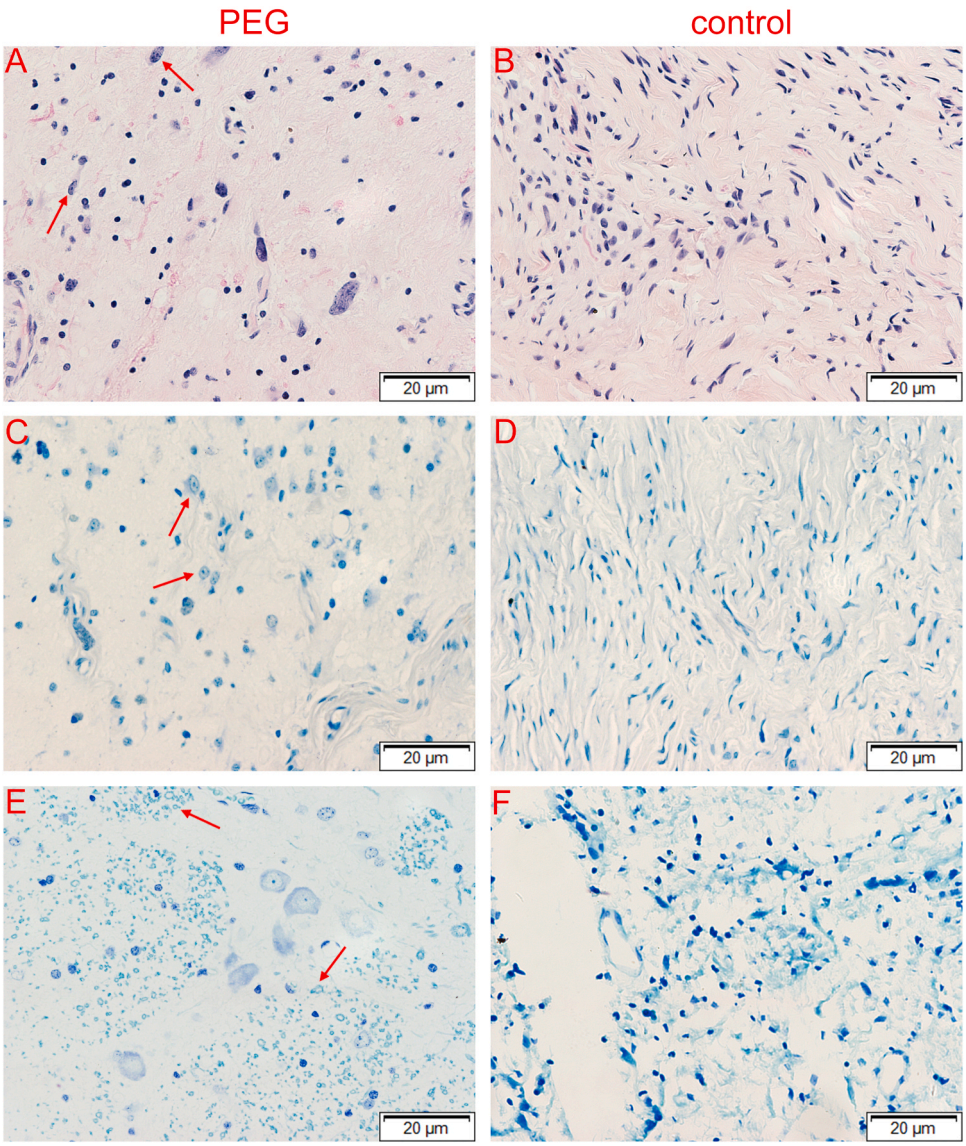

Fig. 4. Optical microscopy at 400x with H&E (A, B), Nissl (C, D) and LFB (E, F) stains. Intact and healthy neuron bodies (arrows in A, C) and myelin tissue (arrows in E) could be observed in PEG-treated animal, but not in the control (B, D, F). Scale bars =20 µm.

transected neuron membranes. Intriguingly, the formation of an astrocytic scar has been shown to promote initial axon regrowth during the earliest stages of SCI; only during the subacute phase, the scar slowly evolves into a nonpermissive state (Rolls et al., 2009; Bradbury and Burnside, 2019; Vangansewinkel et al., 2019). In the present acute SCT model, by the time the scar transitions to its nonpermissive state, neural fibers would have had the opportunity to either re-sprout or fuse across the transection interface, effectively creating a "bridge" between the two stumps. Therefore, PEG administration does not deprive the regrowth opportunity from benefiting the advantageous effects of the early scar formation.

Of particular significance with regard to fusion is the sharpness of the transection, which stands as a crucial determinant for successful axonal regeneration. For instance, a rodent study highlighted that an exceedingly sharp transection yielded edema-free lesions and ultimately avoided the formation of cystic areas or scars. Conversely, a relatively blunt transection led to collateral injury in close proximity to the transection site, leading to edema followed by scar formation and cystic regions around the lesions (Yoshida et al., 2013).

An important point to raise is the dissociation between the rapidity of recovery of neural transmission in the sensory (dorsal) columns (minutes) and the much slower pace of motor recovery (days to weeks). This calls for some clarification. The GEMINI SCF protocol does not achieve its results by re-fusing the almost 20 million of fibers coursing in the white matter (i.e. pyramidal and direct corticospinal fibers), but, as mentioned above, by neuroprotecting gray matter interneurons that belong to a sensori-motor pathway that works in parallel to the more classically understood, long projection fibers. In particular, motor fibers arising from the motor areas in the brain send projections directly to spinal motor neurons, but also simultaneously to a network of propriospinal interneurons that spans the entire length of the brainstem and spinal cord (Canavero, 2015; Canavero et al., 2016). All studies to date, including clinical case reports (Goldsmith et al., 2005; Tabakow et al., 2014) that describe recovery of motor function after spinal cord reconstruction, are explained by positing a driving role of this inter-neuronal system rather than restoration of the long motor fibers in the white matter. In our model too, recovery of motor function starts days after transection and fusion and grows in time, as the fiber substrate of the motor-coded propriospinal pathways is slowly re-established. As is well known, recovery from SCI also involves plastic rearrangements at multiple levels of the CNS, particularly in the brain (Isa and Nishimura, 2014; Isa, 2017) and these take time to occur.

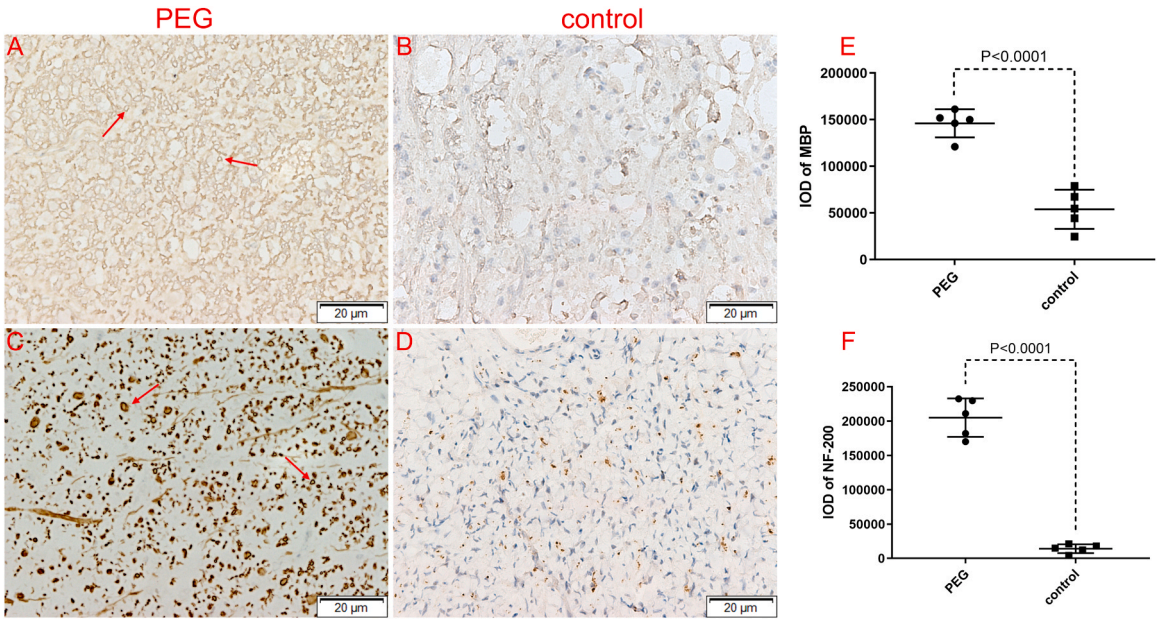

Fig. 5. Immunohistochemical staining of the two monkeys and the positive staining density of NF-200 and MBP. The NF-200-positive axons and MBP-positive myelin sheaths were observed in the PEG-treated monkey (arrows in A, C), while almost absent in the control (B, D). The positive staining densities of NF-200 and MBP in the PEG-treated monkey were significantly higher than those in the control, with a statistically significant difference ($p < 0.05$) (E, F). Scale bars =20 μm.

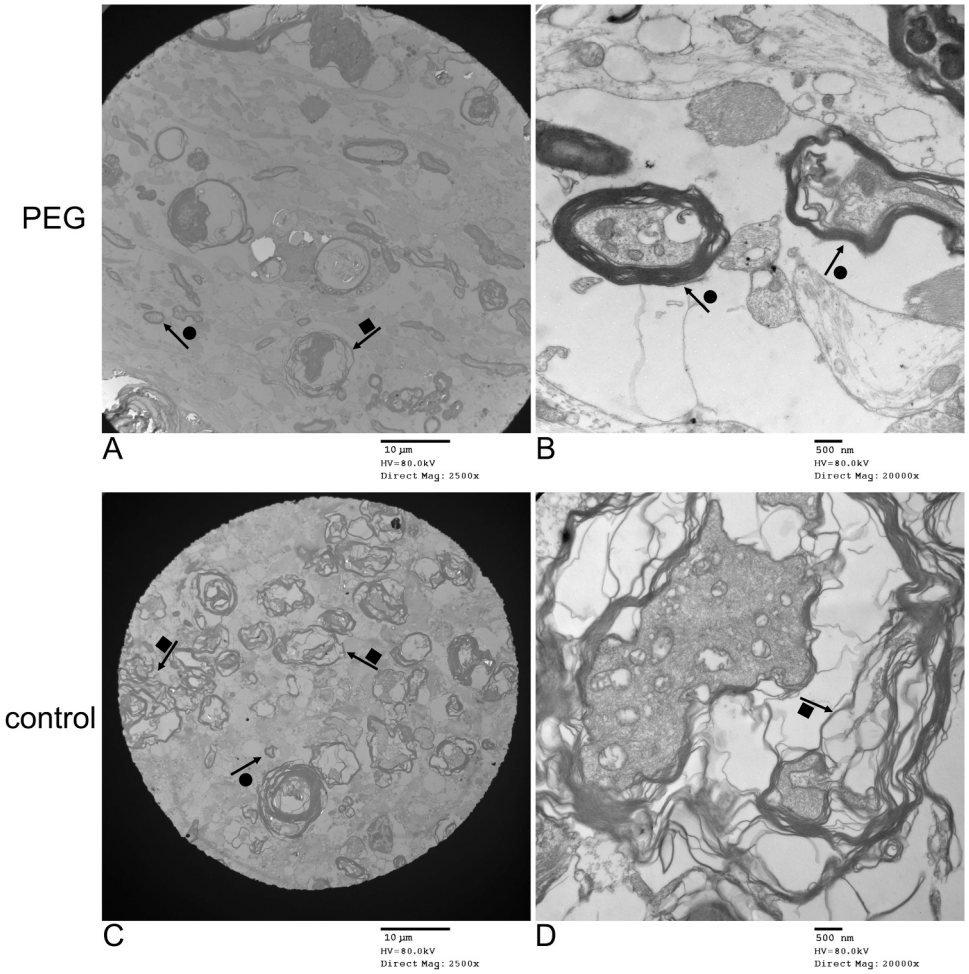

Fig. 6. Representative images of TEM of the two monkeys. More newly myelinated tissue and less disorganized myelination were observed at the transection site of the PEG-treated monkey (A, B). In contrast, the control monkey showed more disorganized myelination and less newly myelinated tissue (C, D). Scale bars =10 μm in (A, C); 500 nm in (B, D).

In more detail, rapid (minutes) recovery of cSSEPs after complete SCT in the present case (Fig. 2) as in our previous rodent and canine studies (Ye et al., 2016; Ren et al., 2017; Liu et al., 2018) provides objective neurophysiologic evidence of the actual fusion of long fibers at the level of the dorsal columns, which are packed and compact, just like peripheral nerves, where PEG fusion is well established. On the other hand, descending pyramidal fibers (about 1 million) do not form (unlike what appears in standard textbooks) a uniform bundle, but fan out and are intermixed in the white matter, hampering effective pyramidal motor fiber-on-pyramidal motor fiber fusion. Since movement is actually driven by the gray matter propriospinal pathway (Canavero et al., 2016), fusion of pyramidal fibers does not appear to be necessary, contrary to standard teaching.

The experimental animals in this study were not submitted to any special form of neurorehabilitation, in particular no electrical stimulation of the fusional area to accelerate sprouting across the interface, which is believed to be important in and integral to integral to the GEMINI SCF protocol (Canavero and Ren, 2016). Ever since the pioneering work of Dimitrijevic and colleagues in the 1990's (Dimitrijevic et al., 1998), spinal cord stimulation, along with intensive rehabilitation, has emerged as a promising technique to help some SCI patients re-acquire some level of motor function (Angeli et al., 2018; Calvert et al., 2019). Combining PEG with spinal cord stimulation is expected to accelerate and further improve recovery, which would also include sensory function; initial rodent data point in that direction (unpublished observations).

A substantial proportion, up to 40 %, of individuals afflicted by SCI contend with a debilitating and chronic pain condition known as central pain of spinal cord origin. This affliction attributes its pathophysiological underpinnings to anomalous generators located within the damaged gray matter both at and above the level of injury. Selectively silencing these generators through interventions like extended dorsal root entry zone coagulations has demonstrated efficacy in alleviating pain in some of these patients (Canavero and Bonicalzi, 2018; Falci et al., 2018). It is within the realm of feasibility to posit that alleviation of this pain can be achieved through the excision of the most severely damaged portion of the spinal cord. Remarkably, the PEG-treated monkey did not appear to show any signs of such pain throughout the entire postoperative duration, extending up to the 18-month follow-up.

Additionally, an intriguing observation emerged from this study: the monkeys exhibited a preference for a seated position, distinct from the prone position favored by the beagle dogs in our prior study. This behavioral inclination of the monkeys engendered the development of kyphosis in both subjects following the surgical removal of the T10 lamina (Fig. 3 A1-D1). Notably, the control monkey, in particular, engaged in prolonged sitting periods due to the absence of motor function recovery in its hind limbs. It is notable that the angle of kyphosis in the control monkey just one month after surgery has already surpassed that in the PEG-treated monkey at the 18-month (Fig. 3 A1, D1). Importantly, both humans and monkeys share similar behavioral tendencies. Derived from the findings of this study, we propose the imperative of attending to spinal stability during the clinical translation of PEG treatment for SCI. Consequently, the application of an internal fixation system or postoperative thoracolumbar fixation brace following laminectomy is recommended to prevent kyphosis.

This study comes with certain limitations. The spinal cord injury model used in this monkey experiment was an acute complete transection model, which is extremely rare in clinical cases. However, non-human primate experiments are essential prior to clinical translation. Furthermore, we conducted a thorough investigation into the impact of PEG on spinal cord fusion using surgical models, including transplantation of the vascularized pedicle of hemisected spinal cord (Ren et al., 2021) and vascularized allograft spinal cord transplantation (Shen et al., 2024) in Beagle models. Both this study and our previous research involving Beagle surgical models provide robust evidence supporting the clinical translation of PEG. In conclusion, this study confirms that a completely transected spinal cord can be treated with the neuroprotectant fusogen to allow restoration of sensorimotor function in a primate model.

Ethical approval

All procedures conducted in this study received approval from both the Institutional Animal Care and Use Committee of Harbin Medical University (HMUIRB-2008–06).

Funding

This work was supported by the National Natural Science Foundation of China (grant numbers 82060874) and the Science and Technology Department of Guangxi Zhuang Autonomous Region (grant numbers Guike AB21196062).

CRediT authorship contribution statement

Mingzhe Zhang: Methodology, Investigation. **Zehan Liu:** Writing – review & editing, Project administration, Methodology, Investigation. **Shuai Ren:** Writing – original draft, Validation, Methodology, Investigation. **Weihua Zhang:** Writing – original draft, Validation, Methodology, Investigation, Formal analysis, Data curation. **Xiaoping Ren:** Writing – review & editing, Supervision, Project administration, Methodology, Funding acquisition, Conceptualization. **Junfeng Xu:** Methodology, Investigation. **Xiangchen Guan:** Methodology, Investigation.

Declaration of Competing Interest

The authors declare that they have no known competing financial interests or personal relationships that could have appeared to influence the work reported in this paper.

Data availability statement

The data that support the findings of this study are available from the corresponding author upon reasonable request.

References

Ahuja, C.S., Wilson, J.R., Nori, S., et al., 2017. Traumatic spinal cord injury. Nat. Rev. Dis. Prim. 3, 17018.
Angeli, C., Boakye, M., Morton, R., et al., 2018. Recovery of Over-Ground Walking after Chronic Motor Complete Spinal Cord Injury. N. Engl. J. Med. 379, 1244–1250.
Bradbury, E.J., Burnside, E.R., 2019. Moving beyond the glial scar for spinal cord repair. Nat. Commun. 10, 3879.
Calvert, J., Grahn, P., Zhao, K., Lee, K., 2019. Emergence of epidural electrical stimulation to facilitate sensorimotor network functionality after spinal cord injury. Neuromodulation: J. Int. Neuromodulation Soc. 22, 244–252.
Canavero, S., 2015. The "Gemini" spinal cord fusion protocol: Reloaded. Surg. Neurol. Int 6, 18.
Canavero, S., Bonicalzi, V., 2018. Central Pain Syndrome. Springer.
Canavero, S., Ren, X., Kim, C.Y., Rosati, E., 2016. Neurologic foundations of spinal cord fusion (GEMINI). Surgery 160, 11–19.
Canavero, S., Ren, X.-P., 2016. The Spark of Life: Engaging the Cortico-Truncoreticulo-Propriospinal Pathway by Electrical Stimulation. CNS Neurosci. Ther. 22, 260–261.
Dimitrijevic, M., Gerasimenko, Y., Pinter, M., 1998. Evidence for a spinal central pattern generator in humans. Ann. N. Y. Acad. Sci. 860, 360–376.
Falci, S., Indeck, C., Barnkow, D., 2018. Spinal cord injury below-level neuropathic pain relief with dorsal root entry zone microcoagulation performed caudal to level of complete spinal cord transection. J. Neurosurg. Spine 28, 612–620.
Goldsmith, H.S., Fonseca Jr., A., Porter, J., 2005. Spinal cord separation: MRI evidence of healing after omentum-collagen reconstruction. Neurol. Res 27, 115–123.
Institute of Laboratory Animal Resources (U.S.). Committee on Pain and Distress in Laboratory Animals. Recognition and alleviation of pain and distress in laboratory animals. Washington, D.C.: National Academy Press; 1992.
Isa, T., 2017. The Brain Is Needed to Cure Spinal Cord Injury. Trends Neurosci. 40, 625–636.
Isa, T., Nishimura, Y., 2014. Plasticity for recovery after partial spinal cord injury - hierarchical organization. Neurosci. Res 78, 3–8.

Kim, C.Y., Oh, H., Ren, X., Canavero, S., 2017. Immunohistochemical evidence of axonal regrowth across polyethylene glycol-fused cervical cords in mice. Neural Regen. Res 12, 149–150.
Liu, Z., Ren, S., Fu, K., et al., 2018. Restoration of motor function after operative reconstruction of the acutely transected spinal cord in the canine model. Surgery 163, 976–983.
Luo, J., Borgens, R., Shi, R., 2002. Polyethylene glycol immediately repairs neuronal membranes and inhibits free radical production after acute spinal cord injury. J. Neurochem. 83, 471–480.
Pasut, G., Panisello, A., Folch-Puy, E., et al., 2016. Polyethylene glycols: An effective strategy for limiting liver ischemia reperfusion injury. World J. Gastroenterol. 22, 6501–6508.
Ren, X., Kim, C.Y., Canavero, S., 2019b. Bridging the gap: Spinal cord fusion as a treatment of chronic spinal cord injury. Surg. Neurol. Int. 10, 1–24.
Ren, S., Liu, Z., Kim, C.Y., et al., 2019a. Reconstruction of the spinal cord of spinal transected dogs with polyethylene glycol. Surg. Neurol. Int 10, 50.
Ren, S., Liu, Z.H., Wu, Q., et al., 2017. Polyethylene glycol-induced motor recovery after total spinal transection in rats. CNS Neurosci. Ther. 23, 680–685.
Ren, S., Zhang, W., Liu, H., et al., 2021. Transplantation of a vascularized pedicle of hemisected spinal cord to establish spinal cord continuity after removal of a segment of the thoracic spinal cord: A proof-of-principle study in dogs. CNS Neurosci. Ther.
Rolls, A., Shechter, R., Schwartz, M., 2009. The bright side of the glial scar in CNS repair. Nat. Rev. Neurosci. 10, 235–241.
Rosenzweig, E.S., Brock, J.H., Lu, P., et al., 2018. Restorative effects of human neural stem cell grafts on the primate spinal cord. Nat. Med 24, 484–490.
Shen, T., Zhang, W., Lan, R., et al., 2024. Developing preclinical dog models for reconstructive severed spinal cord continuity via spinal cord fusion technique. IBRO Neurosci. Rep. 16, 560–566.
Sledge, J., Graham, W.A., Westmoreland, S., et al., 2013. Spinal cord injury models in non human primates: are lesions created by sharp instruments relevant to human injuries? Med Hypotheses 81, 747–748.
Tabakow, P., Raisman, G., Fortuna, W., et al., 2014. Functional regeneration of supraspinal connections in a patient with transected spinal cord following transplantation of bulbar olfactory ensheathing cells with peripheral nerve bridging. Cell Transpl. 23, 1631–1655.
Vangansewinkel, T., Lemmens, S., Geurts, N., et al., 2019. Mouse mast cell protease 4 suppresses scar formation after traumatic spinal cord injury. Sci. Rep. 9, 3715.
Ye, Y., Kim, C.Y., Miao, Q., Ren, X., 2016. Fusogen-assisted rapid reconstitution of anatomophysiologic continuity of the transected spinal cord. Surgery 160, 20–25.
Yoshida, Y., Kataoka, H., Kanchiku, T., et al., 2013. Transection method for shortening the rat spine and spinal cord. Exp. Ther. Med 5, 384–388.